

# Mercury vapor analyzer based on capillary lamp with natural mercury isotope composition in the transverse Zeeman effect: capabilities and prospects

V V Tatur and A A Tikhomirov

Institute of Monitoring of Climatic and Ecological Systems SB RAS, Tomsk, 634055, Russia

E-mail: tatur@imces.ru; tikhomirov@imces.ru

**Abstract.** A mercury-vapor analyzer which is based on a method of atomic absorption spectroscopy is proposed to operate in the atmospheric air. The source of emission used in the instrument is a low-pressure capillary lamp filled with mercury of natural isotope composition. Features of its emission spectrum are described under the transverse Zeeman effect in the vicinity of a resonance wavelength of 253.7 nm. The emission intensities  $\pi$  and the sums of  $\sigma$  components of this lamp are studied. The results of experimental investigations of the analyzer operating modes are presented, and systematic measurement errors are estimated ( $\pm 30$  ng/m<sup>3</sup>). Some options of improving the analyzer response are demonstrated.

## 1. Introduction

The commercial portable gas analyzers RGA-11 [1] and RA-915+ [2] which measure mercury vapor concentration in the atmospheric air are based on the method of differential optical absorption. In order to generate two wavelengths in them:  $\lambda_{on}$  (on the absorption line of the substance being examined) and  $\lambda_{off}$  (off the absorption line), a low-pressure capillary mercury lamp (CML) filled with the <sup>204</sup>Hg mercury isotope is used, which emits in the UV range (at  $\lambda_0 \cong 253.7$  nm). For this the CML is placed in a magnetic field, and the longitudinal Zeeman effect is utilized [3]. Two radiation components are generated in this case: one with right  $\sigma^+$  and the other with left  $\sigma^-$  circular polarizations. For the magnetic induction  $B \cong 0.4$  T, the  $\sigma^+$ -component ( $\lambda_{on}$ ) is found near the maximum of the natural mercury absorption band, while the  $\sigma^-$ -component ( $\lambda_{off}$ ) is found at the band absorption edge [1, 2].

The long-time practice of applying such devices has revealed their major limitation: an insufficient long-term stability of their metrological characteristics resulting from an uncontrollable temporal drift of the CML emission parameters and the optical signal detection system. Among the other disadvantages is the use of expensive components in their design: a photo-elastic polarization modulator converting the circular  $\sigma$ -components into a linear one and an isotope-filled lamp. More recently an experimental prototype DOG-05 analyzer [4, 5] has been developed at IMCES SB RAS (Tomsk, Russia), which is based on the transverse Zeeman effect [3], wherein all three components splitting the <sup>204</sup>Hg isotope emission line are implemented:  $\pi$ -,  $\sigma^+$ -, and  $\sigma^-$ -components possessing linear polarization. Note that the  $\pi$ -component persists in the center of the absorption band contour of the natural mercury isotopes, and both  $\sigma$ -components are found at its edges (at  $B \cong 1$  T). This has simplified the optical layout of the device by removing the photo-elastic polarization modulator [5].

In order to remove the limitations of the isotope-filled CML, an experimental prototype has been designed, an RGA/m atmospheric mercury vapor analyzer relying on a lamp filled with mercury of a natural isotope mixture (NIM) [6]. This work reports the features and results of operation of this device.



## 2. Hyperfine structure of spectral lines of CML with NIM in the transverse Zeeman effect

A special feature of the CML emission spectrum with a NIM in a magnetic field is the availability of a hyperfine structure due to the complex isotopic mixture. A sample spectrum structure calculated by M. A. Buldakov in 2012 is presented in Figure 1. The calculation included the percentages of isotopes in natural mercury with the following nuclear masses: 196 (0.15 %), 198 (9.97), 199 (16.87), 200 (23.1), 201 (13.18), 202 (29.86), and 204 (6.87) [7]. It was also taken into account that the odd-mass isotopes ( $^{199}\text{Hg}$  and  $^{201}\text{Hg}$ ) having fractional nuclear spins (1/2 and 3/2, respectively) and the negative parity contribute to different parts of the total absorption line band contour of the isotope mixture. The Lorentz half-width of the isotope emission line was assumed in the calculations of the spectrum to be  $0.03\text{ cm}^{-1}$ . The spectral line of the  $^{202}\text{Hg}$  isotope, whose percentage in the atmospheric mercury is the highest, was taken as a zero reference point in the calculations. The first line in the  $\sigma$ -component spectrum corresponds to the emission isotopes 199a, 204, and 201a, the second one to 202, the third one to 200, the fourth one to 201b and 198, and the fifth one to 199b (from left to right). In the magnetic fields with  $B \geq 1\text{ T}$ , the  $\pi$ -components of the odd isotopes 199a, 199b, 201a, 201b, and 201c shift towards the region of the  $\pi$ -component of the isotope 200 broadening this line. Thus, the emission spectrum of such a CML must contain four lines for the  $\pi$ -component (Figure 1).

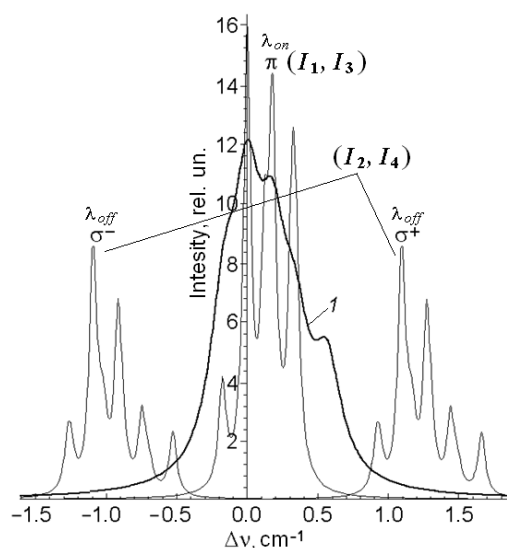


**Figure 1.** Hyperfine structure of emission from a CML filled with NIM mercury in a magnetic field with  $B = 1.56\text{ T}$  in the presence of the transverse Zeeman effect near the resonance line  $\lambda = 253.7\text{ nm}$ :  $I$  – total contour of the emission spectrum of the atmospheric mercury isotope mixture (without the field);  $\pi(\lambda_{on})$  – spectral lines of the  $\pi$ -component emission;  $\sigma^+(\lambda_{off})$  and  $\sigma^-(\lambda_{off})$  – spectral lines of the split  $\sigma$ -component emission.

It is evident from Figure 1 that the emission lines of the  $\sigma^+$ - and  $\sigma^-$ -components at  $B = 1.56\text{ T}$  are practically beyond the NIM mercury absorption contour  $I$ . This allows implementing the differential method, in which case the  $\pi$ -component emission lines ( $\lambda_{on}$ ) are absorbed by the atmospheric mercury vapor, while the emission lines of the  $\sigma$ -component sum lie at the edges of this contour ( $\lambda_{off}$ ).

Theoretically, the intensity of the  $\pi$ -component would be equal to the sum of intensities of the  $\sigma$ -components [3, 7]. It was, however, found in the testing of the RGA/m experimental prototype that in strong magnetic fields (at  $B \geq 0.9\text{ T}$ ), due to the Lorentz force acting on the discharge plasma electrons, the discharge intensity in the transverse and longitudinal sections of the CML capillary becomes inhomogeneous [8, 9]. There is also a marked change in the ratio between the emitted intensities of the  $\pi$ - and  $\sigma$ -components,  $\delta = (I_\sigma - I_\pi)/(I_\sigma + I_\pi)$ . The results of our investigations

demonstrated that the value of  $\delta$  essentially depends on the CML capillary inner diameter, and is practically independent of the induction value  $B$  and variations in the voltage  $U$  exciting a high-frequency discharge in the lamp. We also investigated the influence of the ambient temperature variations within the interval from 15 to 45 °C, which showed that during these variations the value of  $\delta$  was increasing from 5 to 14 %. One of the reasons for this phenomenon is an increase in the percentage of unexcited mercury with increasing temperature, and thus, including self-absorption the fraction of the  $I_\pi$  intensity is decreased.

It follows that when designing a mercury vapor analyzer it is necessary to take into account the initial inequality of the  $\pi$ -component intensities  $I_\pi$  and the sum of intensities of the  $\sigma$ -components  $I_\sigma$ .

### 3. Analyzer RGA/m optical scheme

The optical scheme of the RGA/m instrument is shown in Figure 2. A detailed description of its performance and operation is given elsewhere [6]. The CML was excited with a high-frequency discharge ( $f = 200$  MHz,  $U = 6\div 9$  V) at the magnetic field induction value  $B = 0.92$  T. At this magnetic field the CML performance was quite stable, but splitting of the  $\sigma$ -component spectrum compared to that of the  $\pi$ -component was lower than it is shown in Figure 1; in other words, the  $\sigma^+$  and  $\sigma^-$ -components remained on the slopes of the NIM mercury absorption contour  $I$  (see Figure 1).

The design solution of the RGA/m device provides for an option of receiving four signals  $I_1 \div I_4$  (their corresponding spectral locations are shown in Figure 1), which allow determining the mercury vapor concentration in a measuring cell formed by spherical mirrors  $10 \div 12$ . Signals  $I_1$  and  $I_2$  of the measuring channel pass through the cell, while signals  $I_3$  and  $I_4$ , using deflecting mirrors  $6$  and  $15$  form a reference channel of the analyzer. The design scheme provides for a possibility of equalizing the  $\pi$ -component intensities  $I_\pi$  ( $I_1, I_3$ ) (linearly polarized in the plane of the figure) and the sum of the  $\sigma$ -component intensity  $I_\sigma$  ( $I_2, I_4$ ) (linearly polarized in the perpendicular plane) by varying the tilt angle of compensation plate  $3$  [8]. The data acquisition of this analyzer allows alternatively measure the signal intensities  $I_1 \div I_4$  at a frequency of 400 Hz via rotating elements  $4$  and  $5$  and perform averaging of the results obtained within 2 seconds.

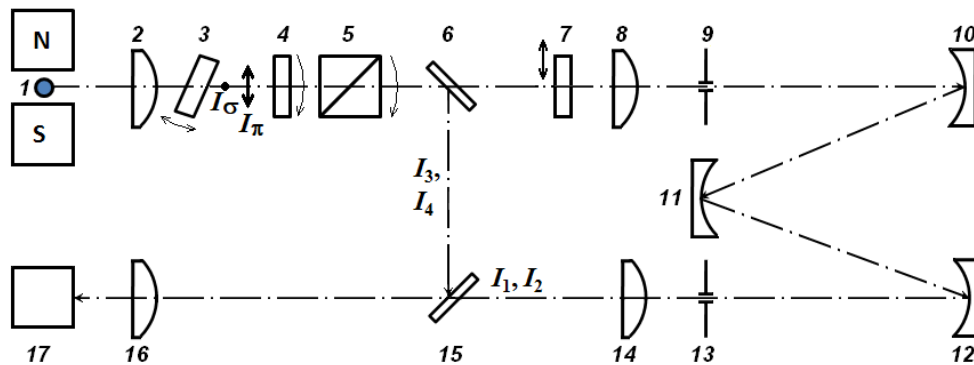


**Figure 2.** Optical scheme of the RGA/m analyzer:  $1$  – CML transverse section in the magnetic field; N, S – magnet poles; 2, 8, 14, 16 – lenses; 3 – polarization compensation plate; 4 – phase plate; 5 – Glan prism; 6, 15 – deflecting mirrors; 7 – etalon cell; 9, 13 – field diaphragms;  $10\div 12$  – spherical mirrors; 17 – photoreceiver.

The measured signal values  $I_1 \div I_4$  allow calculating the mercury vapor concentration  $N_{\text{Hg}}$  in the measuring cell without any preliminary equalization of the intensities  $I_\pi$  and  $I_\sigma$  emitted by the CML.

$$N_{\text{Hg}} = K \ln (I_2 I_3 / I_1 I_4), \quad (1)$$

where  $K$  is the coefficient of proportionality (instrument constant). For RGA/m, the value of  $K$  is of the order of  $n \cdot 10^4$ ; therefore, the uncertainty of measurement of signals  $I_1 \div I_4$  introduces an essential error into the calculated concentration value  $N_{\text{Hg}}$ .

#### 4. Experimental results

The temporal dependences of the four detected signals (without preliminary equalization of their intensity) and the mercury vapor concentrations calculated by formula (1) are presented in Figure 3. The measurements were performed after the CML attained its stable operating performance, 30 min after switching its excitation. The decrease in the intensities  $I_1$  and  $I_2$  in the interval of  $\sim 360 \div 500$  s (Interval 1) is due to the introduction of etalon cell 7 with a known mercury vapor concentration into the measurement channel (see Figure 2). Then,  $\sim 1270$  s after the start of measurements (Interval 2), a small amount of mercury vapor was injected into the measuring cell, which was detected as a change in intensities  $I_1$  and  $I_2$ . The change in the value of  $I_2$  both after the introduction of the etalon cell and upon injected the mercury vapor is attributed to the fact that the magnetic field induction was  $B = 0.92$  T, which (as mentioned above) did not ensure complete displacement of the  $\sigma^+$ - and  $\sigma^-$ -components off the NIM mercury absorption spectrum. In addition, in Interval 1 the decrease in intensities  $I_1$  and  $I_2$  after the introduction of the etalon cell is due to the loss in the quartz glass of the cell itself and to the reflections from its four optical surfaces.

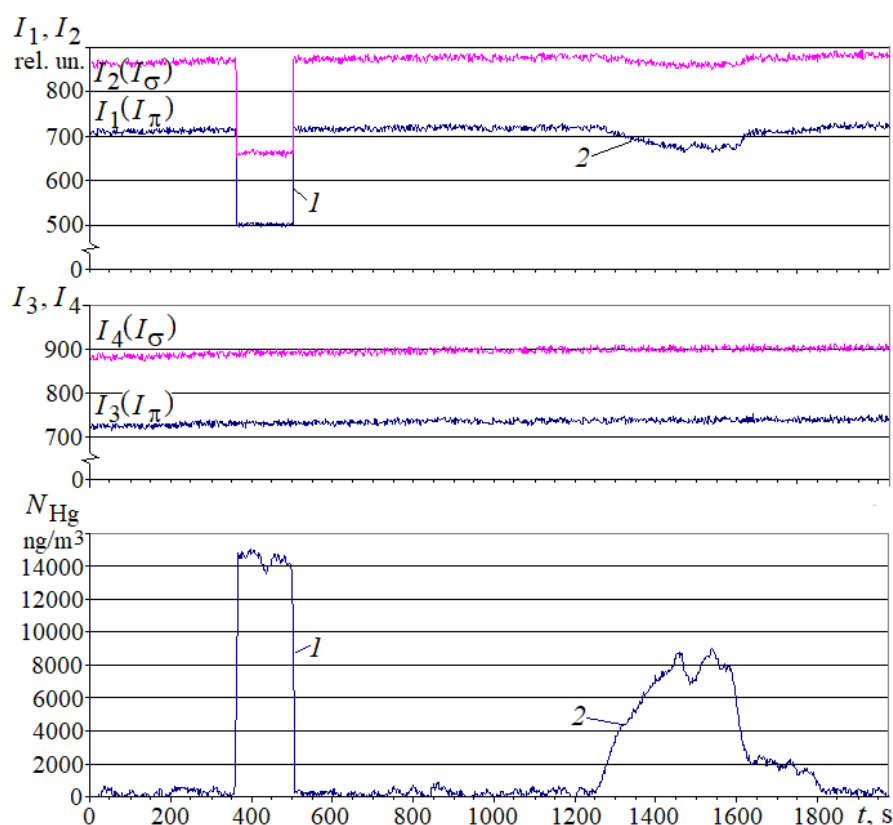


**Figure 3.** Analyzer response to the introduction of etalon cell filled with mercury vapor into the measuring channel (Interval 1) and puffing a small amount of mercury vapor (Interval 2) for the case of non-equalized intensities  $I_\sigma$  and  $I_\pi$  emitted by the CML.

Note also that the initial inequality of intensities  $I_\sigma$  and  $I_\pi$ , emitted by the CML negatively affects the mercury concentration estimates  $N_{\text{Hg}}$  obtained by relation (1). It is evident from Figure 3 that the

intensities  $I_1 \div I_4$  monotonously increase (by approximately 5 %) within the half-hour measurement period. As a result the zero level of the measured concentration  $N_{\text{Hg}}$  drifts. The introduction of an empty etalon cell into the measuring channel is practically always accompanied by a spurious signal. This spurious signal is due to an incomplete compensation of non-selective absorption under this operating mode of the analyzer. Therefore, the systematic error of the measurements by (1) is as large as  $\pm 500 \text{ ng/m}^3$ .

One of the methods for ruling out the zero-level drift of the measured mercury concentration  $N_{\text{Hg}}$  is to equalize the initial values of intensities  $I_\sigma$  and  $I_\pi$ , emitted by the CML. An option of their equalization using a polarization compensation plate 3 is reported elsewhere [8]. Given such equalization, it becomes unnecessary to measure the intensities of the reference channel  $I_3$  and  $I_4$ , and the mercury vapor concentration can be calculated using the following relation:

$$N_{\text{Hg}} = K \ln(I_2/I_1). \quad (2)$$

Figure 4 presents the measurement data obtained using an RGA/m analyzer for the case of preliminary equalized intensities  $I_\sigma$  and  $I_\pi$ . Without the mercury vapor in the measuring cell signals  $I_1$  and  $I_2$  overlap. A number of possible scenarios of the analyzer performance were tested. An empty etalon cell was inserted into the measurement channel within Interval 1 ( $\sim 330 \div 740 \text{ s}$ ). In this case the analyzer recorded an equal decrease in the signal intensities  $I_1$  and  $I_2$ . The calculation by (2) of the mercury concentration  $N_{\text{Hg}}$  in the analyzer data acquisition system indicates the presence of mercury vapor at a systematic error level, which is about  $\pm 30 \text{ ng/m}^3$  (see bottom part of Figure 4).

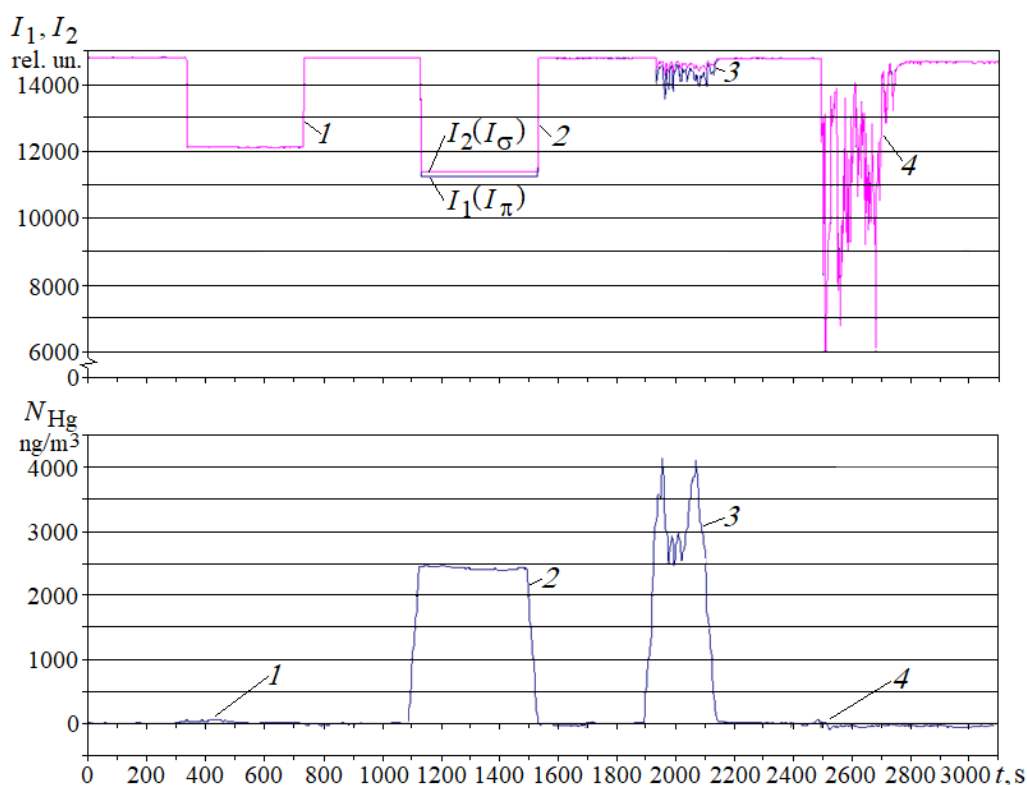


**Figure 4.** Temporal dependences of measured signals and calculated mercury vapor concentrations  $N_{\text{Hg}}$  for different experimental conditions: empty etalon cell (Interval 1,  $\sim 330 \div 740 \text{ s}$ ), etalon cell with mercury (Interval 2,  $\sim 1100 \div 1540 \text{ s}$ ), minor amount of mercury vapor (Interval 3,  $\sim 1920 \div 2140 \text{ s}$ ), smoke (Interval 4,  $\sim 2500 \div 2740 \text{ s}$ ).

Then, in Interval 2 (~1100÷1540 s) an etalon cell filled with mercury vapor was inserted into the measurement channel. In this case, the measured signal intensities  $I_1$  and  $I_2$  were observed to differ from each other by a value proportional to the mercury vapor concentration in the etalon cell. After processing the signals  $I_1$  and  $I_2$  in the data acquisition system from this time interval, the measured mercury concentration  $N_{\text{Hg}}$  was found to be  $2480 \pm 30 \text{ ng/m}^3$ .

Within Interval 3 (~1920÷2140 s), a minor amount of mercury vapor was injected into the measuring cell. The signal processing data demonstrate the mercury vapor concentration measured in this interval (bottom graph, Figure 4). The fluctuations observed in the recorded value of  $N_{\text{Hg}}$  are likely to be due to the mercury vapor diffusion within the cell space.

Next, within Interval 4 (~2500÷2740 s), burning paper smoke was injected into the measuring cell. The intensities of both signals  $I_1$  and  $I_2$  were observed to change to a large extent, while their temporal variations were the same. Upon processing the signals from this interval, the data acquisition system indicated the measured concentration of  $N_{\text{Hg}}$  within the systematic error of  $\pm 30 \text{ ng/m}^3$ . This suggests complete compensation of the nonselective absorption/scattering signal.

## 5. Conclusions

The above-described series of investigations of the operating modes of an RGA/m experimental prototype using a CML with a natural mercury composition as an emission source operating under the conditions of the transverse Zeeman effect including data reported in [8, 9] have demonstrated the following:

1. The emittance intensity  $I_\pi$  is observed to decrease due to self-absorption of the  $\pi$ -component by unexcited mercury atoms in a CML capillary. As a result, the emittance intensity  $I_\pi$  is invariably lower than  $I_\sigma$ , which is the sum of  $\sigma$ -components at the edges of the total contour of the natural isotope mixture mercury absorption spectrum.

2. There are longitudinal and crosswise inhomogeneities of the intensity distributions  $I_\pi$  and  $I_\sigma$  over a CML capillary due to non-uniform discharge plasma distributions in the longitudinal and crosswise sections of the capillary, resulting in different values of self-absorption of the components being emitted.

3. The difference between the intensities  $I_\pi$  and  $I_\sigma$  under various external factors largely depends on the CML temperature and the internal lamp capillary diameter.

4. The intensities  $I_\pi$  and  $I_\sigma$  can be equalized by using different Fresnel coefficients of reflection of orthogonal polarizations of  $\pi$ - and the sum of  $\sigma$ -components from a planar quartz plate placed on the CML emission path.

5. The preliminary equalization of the intensities  $I_\pi$  and  $I_\sigma$  ensures practically complete compensation for a non-selective absorption/scattering signal. Moreover, this eliminates the uncontrollable zero-level drift of the measured mercury vapor concentration. Given the equalized intensities  $I_\pi$  and  $I_\sigma$ , the use of the reference signal in the analyzer becomes unnecessary. This allows reducing the systematic instrument error by more than an order of magnitude (from 500 to 30  $\text{ng/m}^3$ ).

6. An additional improvement of the analyzer sensitivity could be achieved by increasing the magnetic field inductance up to 1.1 ÷ 1.2 T, which would displace the  $\sigma^+$  and  $\sigma^-$ -components still further off the contour of the natural isotopic mercury absorption spectrum and reduce the systematic measurement error.

The above-proposed device can be used as a portable analyzer of atmospheric mercury vapor in environmental monitoring.

## Acknowledgements

This study was performed under SB RAS project no. IX.138.1.3.

**References**

- [1] Antipov A B, Genina E Yu and Golovayskii Yu A 2002 RGA gas analyzer and its application to environmental mercury monitoring *Atmospheric and oceanic optics* **15** (01) 69-73
- [2] Ganeev A A, Sholupov S E, Pupyshev A A, Bol'shakov A A and Pogarev S E 2011 *Atomic-Absorption Analysis: Schoolbook* (Saint Petersburg: Lan') p 304 [in Russian]
- [3] Frish S È 1963 *Optical Spectra of Atoms* (Moscow: State Publishing House of Physico-Mathematical Literature) p 640 [in Russian]
- [4] Azbukin A A, Buldakov M A, Korolev B V, Korolkov V A, Matrosov I I and Tikhomirov A A 2006 Portable optical mercury vapor analyzer in atmospheric air DOG-05 *Prib. Tekh. Èksp.* **6** 142 [in Russian]
- [5] Buldakov M A, Matrosov I I, Tikhomirov A A and Korolev B V 2011 Portable optical mercury vapour analyzer in atmospheric air DOG-05 *Bezopasn Tekhnosf.* **1** 11 [in Russian]
- [6] Abramochkin A I, Korolkov V A, Mutnitsky N G, Tatur V V, and Tikhomirov A A 2015 Portable mercury gas analyzer with a lamp filled with natural mercury isotope mixture *Proc. of SPIE* 9680 96803D-1
- [7] Al'tman È L, Sveshnikov G B, Turkin Yu I and Sholupov S E 1982 Zeeman atomic absorption spectroscopy *J. Appl. Spectr.* **37** 709
- [8] Abramochkin A I, Tatur V V and Tikhomirov A A 2016 Investigation of the  $\pi$ - and  $\sigma$ -components of mercury capillary lamp radiation in the presence of the transverse Zeeman Effect *Russian Physics Journal* **59** 1343
- [9] Abramochkin A I, Tatur V V and Tikhomirov A A 2017 The features of emission from  $\pi$ - and  $\delta$ -components of a mercury capillary lamp with a natural isotopic composition in the transverse Zeeman Effect *Russian Physics Journal* **60** 1262